Transcriptome analysis of *Fenneropenaeus chinensis* (Decapoda: Penaeidae) after low-salinity exposure identifies differentially expressed genes in pathways potentially related to osmoregulation

Jun Liu[1*], Lei Zhang[1], Zhengfei Wang[2], Daizhen Zhang[2], Shiguang Shao[1] & Jie Shen[1*]

[1] Key Laboratory of Biotechnology in Lianyungang Normal College, Lianyungang, China

[2] Jiangsu Key Laboratory for Bioresources of Saline Soils, Jiangsu Provincial Key Laboratory of Coastal Wetland Bioresources and Environmental Protection, Jiangsu Synthetic Innovation Center for Coastal Bio-agriculture, Yancheng Teachers University, Yancheng, China

Key words: *ATP1A*; *AQP4*; Mineral absorption; Vasopressin-regulated water reabsorption

*Corresponding authors

Jun Liu, E-mail: liuj86@live.cn;

Jie Shen, E-mail: baiyueguang_5202@126.com

Abstract

Ability to tolerate low salinity is a key factor affecting the distribution of the Chinese shrimp (*Fenneropenaeus chinensis*). Although previous studies have investigated the mechanisms underlying adaptations to low salinity in some crustaceans, little is known about low-salinity adaptations in *F. chinensis*, particularly at the molecular level. Here, to identify genes potentially associated with the molecular response of *F. chinensis* to low-salinity exposure, we compared the transcriptomes of *F. chinensis* in low-salinity (5 ppt) and normal-salinity (20 ppt) environments. In total, 45,297,936 and 44,685,728 clean reads were acquired from the low-salinity and control groups, respectively. De novo assembly of the clean reads yielded 159,130 unigenes, with an average length of 662.82 bp. Of these unigenes, only a small fraction (10.5% on average) were successfully annotated against six databases. We identified 3,658 differentially expressed genes (DEGs) between the low-salinity group and the control group: 1,755 DEGs were downregulated in the low-salinity group as compared to the control, and 1,903 were upregulated. Of these DEGs, 282 were significantly overrepresented in 38 KEGG (Kyoto Encyclopedia of Genes and Genomes) pathways. Notably, several DEGs were associated with pathways important for osmoregulation, including the mineral absorption pathway (*ATP1A*, Sodium/potassium-transporting ATPase subunit alpha; *CLCN2*, Chloride channel 2; *HMOX2*, Heme oxygenase 2; *SLC40A1/FPN1*, Solute carrier family 40 iron-regulated transporter, member 1), the vasopressin-regulated water reabsorption pathway (*AQP4*, Aquaporin-4; *VAMP2*, Vesicle-associated membrane protein 2; *RAB5*, Ras-related protein Rab-5) and the

ribosome pathway. Our results help to clarify the molecular basis of low-salinity adaptations in *F. chinensis*.

Key words: *ATP1A*; *AQP4*; Mineral absorption; Vasopressin-regulated water reabsorption

Introduction

To improve the low-salinity aquaculture of marine crustaceans, it is necessary to understand their adaptation ability to low salinity and mechanisms used by these organisms to tolerate low-salinity environments. As osmoregulators, some euryhaline marine and brackish crustaceans have a strong ability to adapt to environments with varying salinities (from almost 0 ppt up to 40 ppt) [1-4]. This ability to tolerate low salinity is a key factor affecting the distribution of such crustaceans in low-salinity environments [5-6].

Previous studies have explored the mechanisms underlying low-salinity tolerance in mariculture crustaceans at the organismal, cellular, and molecular levels [1, 7-10]. In general, the most common adaptive strategies for hyperosmoregulation aim to maintain hemolymph osmolarity above that of the ambient medium, both via salt absorption and via permeability reduction (i.e., reducing or limiting water inflow) [3]. However, most euryhaline crustaceans produce isosmotic urine, and thus considerable salt is lost in low-salinity environments [11-12]. Studies of low-salinity tolerance in crustaceans have shown that the gills also participate in osmoregulation. In detailed reviews, Péqueux (1995) and Henry (2012) assessed the specialized functions of gills and gill parts in various crustaceans and showed that both cuticle permeability and the

70 membrane characteristics of the salt-transporting gill epithelial cells were critical to
71 osmoregulation [1, 3]. Some bio-molecules in the gill epithelial cells facilitate salt
72 absorption and may also inhibit of water inflow, possibly compensating for passive
73 salt loss and water gain; these biomolecules include Na^+/K^+-ATPase, K^+ channels, Cl^-
74 channels, carbonic anhydrase, aquaporins (AQPs), and various exchangers (Na^+/NH_4^+,
75 Na^+/H^+, and Cl^-/HCO_3^-) [3, 5, 13-16].

76 The mechanisms underlying low-salinity adaptations in crustaceans have been
77 investigated with respect to salt absorption [1, 3]. However, although the
78 water-permeability of epithelial cells is known to change rapidly based on the
79 properties of some AQPs [17-18], the regulation of water inflow in invertebrates
80 (particularly crustaceans) by AQPs remains unclear [16, 19]. During osmoregulation,
81 it is also important to determine how energy is distributed in response to low salinity;
82 various invertebrates have been shown to consume more energy during
83 osmoregulation [1, 3].

84 The euryhaline Chinese shrimp (*Fenneropenaeus chinensis*), which has an
85 isosmotic point of 25 ppt, is naturally distributed primarily in the Chinese Yellow Sea,
86 the Bohai Sea, and along the western coast of the Korean Peninsula [20-21]. It is an
87 important commercial shrimp along the coasts of China and Korea [20]. As these
88 shrimp are cultured in much lower salinity (under the isosmotic point), they must
89 manage or tolerate substantial changes in water osmolality. In crustaceans similarly
90 exposed to salinity stress (e.g., the swimming crab, *Portunus trituberculatus*; the
91 Chinese crab, *Eriocheir sinensis;* and the Pacific white shrimp, *Penaeus vannamei*),

several genes in pathways potentially associated with adaptations to low salinity have been reported [22-25]. Reports showed that *F. chinensis* has a poorer ability to maintain a stable hemolymph osmolarity (reflecting the weaker low-salinity adaptation), compared to *P. vannamei* [21, 26]. The poorer ability limits the farming development of *F. chinensis*. However, to date, studies on low-salinity adaptation in *F. chinensis* are still lacking on molecules. Recently Li (2019b) reported on *F. chinensis* that the group after exposure at low salinity (10 ppt) showed significantly elevated citrate synthase (CS) and cytochrome C oxidase (COX) activities in its gill when compared with the group subjected to 20 ppt salinity condition [21]. For this species, these proteins have also included Na^+/K^+-ATPase, phenoloxidase (PO), heat shock proteins (HSPs), ion-transport enzymes [27-29].

In addition, here, we hypothesize that several other proteins, including channel transporters, AQPs, and proteins associated with energy consumption, are involved in low-salinity resistance in *F. chinensis*. To test this hypothesis, we aimed to use transcriptome analysis to identify and annotate the genes differentially expressed in *F. chinensis* exposed to low-salinity conditions, and to explore the molecular pathways associated with osmoregulation or energy consumption that were overrepresented in these genes. Our results will clarify the mechanisms underlying low-salinity tolerance in *F. chinensis* and further help to explain the adaptation ability during osmoregulation in this species.

Materials and Methods

Sample collection and treatment

Live shrimp were obtained from a local market near their farm of origin (in Lianyungang, N 34°48'52.47", E 119°12'19.08"). Shrimp were transported to our laboratory at Lianyungang Normal College. Before experimentation, all shrimp were acclimated to a salinity of 20 ppt at 25ºC for 5 days. This salinity was similar to the natural isosmotic point of this species (25 ppt) [20, 30], as well as to the salinity at the shrimp farm (23 ppt). At late stage of the acclimation period, survival rates were consistently high. We then randomly divided the shrimp into two groups (n = 20 per group) by two 22 L (liters) of transparent plastic tanks: the low-salinity group (LS) was exposed to low salinity levels (5 ppt) for 24 h, while the control group remained at 20 ppt salinity as salinities ranging from 20 to 32 ppt are considered optimal survival rates [20]. *F. chinensis* in this salinity range (20 to 32 ppt) should suffer less salinity stress. In the study, salinity was maintained using sea salt and pure water and measured by a portable salinity meter (Arcevoos® ST6). In each tank, 15 L of water was used and one-third of it was replaced every 12 hours (7:00-19:00). At the end of the 24 h experimental period, the gills of three randomly selected surviving individuals per group (mean body length: 9.13 ± 0.47 cm; mean body weight 5.13 ± 0.65 g) were harvested and stored at -70°C for transcriptome and real-time quantitative PCR (RT-qPCR) analysis.

RNA isolation, library construction, and sequencing

Total RNA was extracted using TRIzol reagent (Invitrogen Corp., USA). RNA concentration was measured using a NanoDrop 2000 spectrophotometer (Thermo Scientific, USA), and RNA integrity was assessed using 1.5% agarose gel

electrophoresis. Magnetic oligo (dT) beads were used to isolate mRNA from total RNA. The mRNA was then fragmented into fragments approximately 200 bp long using fragmentation buffer (Tris-acetate, KOAc, and MgOAc) at 94°C for 35 min. The fragmented mRNA was used to construct the cDNA libraries. At least 5 μl of mRNA solution (≥ 200 ng/μl) was used to construct each library. Sequencing libraries for each sample were generated using the TruSeq RNA Sample Prep Kit (Illumina, USA). Libraries were paired-end sequenced using a HiSeq X Ten platform (Illumina, USA). The read length was 200bp.

Transcriptome assembly and unigene annotation

Raw sequence data were processed using FastqStat.jar V1.0 [31], with default parameters. We then used Cutadapt v1.16 (http://cutadapt.readthedocs.io; [32]) with parameters -q 20 -m 20 to clean the raw sequence data by deleting adapter sequences, deleting poly-N sequences, trimming low-quality sequence ends (<Q20), deleting sequences with N ratios >10%, and removing reads less than 25 bp long. We used Trinity (http://trinityrnaseq.github.io; [33]) to assemble the clean reads. Subsequently, paired-end reads were used to fill the gaps when sequence scaffolds could not be extended on either end. These sequences were defined as transcripts and were subsequently assembled into unigenes based on clustering patterns using Corset [24, 34].

The identified unigenes were annotated against six databases: NCBI nonredundant protein sequences (NR), Protein Families (PFAM), Search Tool for the Retrieval of Interacting Genes (STRING), KEGG (Kyoto Encyclopedia of Genes and

158 Genomes) Ortholog (KO), Gene Ontology (GO), and SWISS-PROT. We searched the
159 unigenes against these databases using BlastX v2.2.25 [35] with a cutoff E-value of
160 10^{-5}. Functional unigenes were classified based on GO terms using Blast2GO
161 (http://www.blast2go.com/b2ghome) [36].

162 Identification and enrichment of differentially expressed
163 unigenes (DEGs)

164 We used Kallisto v0.43.1 (http://kallisto.com) to evaluate the expression levels of
165 the unigenes based on transcripts per kilobase million (TPM) values; higher TPM
166 values reflect higher levels of unigene expression [37]. We used edgeR v3.24 to
167 identify unigenes where |log2 fold-change (FC)| was >1 and the false discovery rate
168 (FDR) was <0.05 [38-39]; these unigenes were considered DEGs. We then identified
169 the KEGG pathways significantly enriched in the DEGs ($P < 0.05$) using
170 hypergeometric test [40].

171 Verification of DEGs using RT-qPCR

172 We selected four RNA-Seq DEGs (three upregulated and one downregulated) for
173 RT-qPCR validation, which belong to the significant pathways (Glycine, serine and
174 threonine metabolism, Mineral absorption and Glycolysis/Gluconeogenesis). We used
175 the *β-actin* gene as the internal reference gene, against which to normalize the
176 expression levels of the target genes. Gene-specific primers were designed based on
177 sequences derived from the transcriptome assembly and annotation using Primer
178 Premier 5.0 [41] (Table 1). Each RT-qPCR (25 µl) contained 12.5 µl of 2 × SYBR
179 qPCR Mix, 1 µl each of forward and reverse primers, 1 µl of cDNA, and 10.5 µl of

RNase-free H_2O. RT-qPCRs were performed on an Applied Biosystems 7500 Real-time PCR system (Applied Biosystems, Thermo Fisher Scientific, Waltham, MA, USA), with the following cycling conditions: an initial denaturation step of 3 min at 95°C; 40 cycles of 15 s at 94°C, 15 s at 55°C, and 25 s at 72°C; and a standard dissociation cycle. Three technical replicates were performed per gene, and the 2–ΔΔCT method [42] was used to calculate relative expression levels. We considered genes differentially expressed between groups if |log2FC| was >1 and the FDR was <0.05.

Table 1. Primers used for real-time quantitative PCR.

Gene name	Forward primer sequence (5'-3')	Reverse primer sequence (5'-3')
β-actin	GCGAGAAATCGTGCGTGAC	AGGGTGCGAGGGCAGTGAT
ATP1A	AGAAGGCCGATATTGGTG	CAGGGATGTTAGATGTCAGG
CLCN2	AACAACACCCATTGCCTCAC	TCCACCAACTCCCAGACG
HK	GCAGACGCAGTTGACGAT	ACTCCTTGGCGAGACCTT
glyA	ACAAATCTGCCCTGAATC	CCTTGAACTCTGCGTCTC

Results

Sequence quality and de novo assembly

After filtering the raw reads, we obtained 45,297,936 clean reads for group LS and 44,685,728 for the control group. Base call accuracy was acceptable based on Q20 values, which correspond to a 99% accuracy rate for each nucleotide base (i.e., A,

C, T and G) in a sequence ([43]: 97.64% and 97.16% of the bases in the LS and control groups, respectively, had quality scores >20 (Q20) (Table 2). De novo assembly yielded 211,955 transcripts and 159,130 unigenes. The average lengths of the transcripts and unigenes were 1,028.64 bp and 662.82 bp, respectively. The N50 values (length of the smallest transcript/unigene in the set that contains the fewest (largest) transcripts/unigenes whose combined length represents at least 50% of the assembly) [44] for the transcripts and unigenes were 2,503 bp and 1,004 bp, respectively (Table 3). The raw data have been uploaded to SRA database and the BioProject ID is PRJNA669213.

Table 2. Clean-read statistics.

Group	Total reads	Total bases	Error%	Q20%	GC%
Low-salinity (LS)	45,297,936	6,725,104,745	0.03	97.14	45.99
Control	44,685,728	6,634,797,034	0.03	97.16	47.40

Table 3. De novo assembly statistics.

Type	Unigenes	Transcripts
Total sequence num	159,130	211,955
Total sequence base	105,474,756	218,024,931
Percent GC	42.42	43.36
Largest (bp)	38,633	38,633
Smallest (bp)	201	186
Average (bp)	662.82	1028.64
N50	1,004	2,503
N90	269	341

Annotation and classification of the transcriptome

We were able to annotate only a small fraction of the 159,130 unigenes against the six databases (10.50% on average). The greatest proportion of unigenes (13.99%; 22,256 unigenes) was annotated against the NR database, followed by the STRING and SWISS-PROT databases (10.89% and 10.94%, respectively; Table 4). GO analysis of the annotated unigenes showed that, in the biological process category, the three terms annotated in the most unigenes were macromolecule metabolic process (10,578 unigenes), organonitrogen compound metabolic process (10,297 unigenes), and regulation of cellular process (9,871 unigenes); in the cellular components category, the three terms annotated in the most unigenes were intracellular (14,934 unigenes), intracellular part (14,883 unigenes), and cytoplasm (14,078 unigenes); and in the molecular function category, the three terms annotated in the most unigenes were cation binding (5,800 unigenes), nucleic acid binding (5,521 unigenes), and anion binding (5,322 unigenes) (Fig 1).

Table 4. Annotation statistics of 159 130 Unigenes on *F. chinensis*.

Database	No. of unigenes	% of total
GO	16,578	10.42%
KEGG	13,975	8.78%
NR	22,256	13.99%
PFAM	13,360	8.40%
STRING	17,325	10.89%
SWISS-PROT	16,700	10.49%
Average	16,699	10.50%

DEG identification and enrichment

We identified 3,658 unigenes as DEGs (i.e., |log2FC |>1 and FDR < 0.05). Of

these, 1,755 were downregulated in the LS group as compared to the control, and 1,903 were upregulated (Fig 2). We identified 38 KEGG pathways as significantly enriched in the 3,658 DEGs ($P < 0.05$, Fig 3). Of these, 13 were metabolic pathways, including tryptophan metabolism, lysine degradation, drug metabolism-cytochrome P450, and tyrosine metabolism; 13 were organismal systems pathways, including salivary secretion, insulin secretion, proximal tubule bicarbonate reclamation, and the TOLL and IMD signaling pathways; and two were cellular process pathways, namely phagosome and regulation of the actin cytoskeleton (Fig 3). The remaining 10 pathways were associated with environmental information processing, drug development, and human diseases (Fig 3). Across all 38 pathways, three were potentially related to osmoregulation: mineral absorption (ko04978), four DEGs; vasopressin-regulated water reabsorption (KEGG: ko04962), three DEGs; and ribosome (ko03010), 29 DEGs (Table 5). The DEGs in these pathways included *ATP1A* (Sodium/potassium-transporting ATPase subunit alpha), *CLCN2* (Chloride channel 2), *VAMP2* (Vesicle-associated membrane protein 2), and *AQP4* (Aquaporin-4), *HMOX2* (Heme oxygenase 2), *SLC40A1/ FPN1* (Solute carrier family 40 (iron-regulated transporter), member 1), *RAB5* (Ras-related protein Rab-5), etc. (Table 5).

Table 5. Unigenes in osmoregulation-related pathways differentially expressed in response to low salinity. OS: Organismal Systems; GIP: Genetic Information Processing

Gene Symbol	Up/Down-regulation (log2FC), LS	Description	KEGG ID

	vs Control		
Mineral absorption-KEGG pathway (OS)			
ATP1A	Upregulated (2.49)	Sodium/potassium-transporting ATPase subunit alpha	ATPase
CLCN2	Upregulated (1.87)	Chloride channel 2	ClC-2
HMOX2	Upregulated (1.10)	Heme oxygenase 2	HMOX
SLC40A1/ FPN1	Downregulated (-1.18)	Solute carrier family 40 (iron-regulated transporter), member 1	FPN1
Vasopressin-regulated water reabsorption- KEGG pathway (OS)			
AQP4	Downregulated (-1.14)	Aquaporin-4;	AQP4
RAB5	Downregulated (-1.26)	Ras-related protein Rab-5	Rab5
VAMP2	Downregulated (-1.20)	Vesicle-associated membrane protein 2	VAMP2
Ribosome- KEGG pathway (GIP)			
RP-L40e	Upregulated (1.30)	Large subunit ribosomal protein L40e	L40e
RP-L36	Upregulated (1.22)	Large subunit ribosomal protein L36e	L36e
RP-L7	Upregulated (1.21)	Large subunit ribosomal protein L7/L12	L7/L12
RP-S3e	Downregulated (-1.10)	Small subunit ribosomal protein S3e	S3e
RP-S4e	Downregulated (-1.03)	Small subunit ribosomal protein S4e	S4e
RP-S9	Downregulated (-1.57)	Small subunit ribosomal protein S9	S9
RP-S14e	Downregulated (-1.06)	Small subunit ribosomal protein S14e	S14e
RP-S15e	Downregulated (-1.13)	Small subunit ribosomal protein S15e	S15e
RP-S15Ae	Downregulated (-1.20)	Small subunit ribosomal protein S15Ae	S15Ae
RP-S19e	Downregulated (-1.07)	Small subunit ribosomal protein S19e	S19e
RP-S21e	Downregulated (-1.38)	Small subunit ribosomal protein S21e	S21e
RP-S23e	Downregulated (-1.06)	Small subunit ribosomal protein S23e	S23e
RP-S27e	Downregulated (-1.24)	Small subunit ribosomal protein S27e	S27e

RP-S29e	Downregulated (-1.06)	Small subunit ribosomal protein S29e	S29e
RP-L5e	Downregulated (-1.10)	Large subunit ribosomal protein L5e	L5e
RP-L7e	Downregulated (-1.05)	Large subunit ribosomal protein L7e	L7e
RP-L9e	Downregulated (-1.27)	Large subunit ribosomal protein L9e	L9e
RP-L10Ae	Downregulated (-1.15)	Large subunit ribosomal protein L10Ae	L10Ae
RP-L13e	Downregulated (-2.71)	Large subunit ribosomal protein L13e	L13e
RP-L14e	Downregulated (-1.00)	Large subunit ribosomal protein L14e	L14e
RP-L17e	Downregulated (-1.10)	Large subunit ribosomal protein L17e	L17e
RP-L18e	Downregulated (-1.40)	Large subunit ribosomal protein L18e	L18e
RP-L21e	Downregulated (-1.07)	Large subunit ribosomal protein L21e	L21e
RP-L23e	Downregulated (-2.59)	Large subunit ribosomal protein L23e	L23e
RP-L28e	Downregulated (-1.07)	Large subunit ribosomal protein L28e	L28e
RP-L29e	Downregulated (-1.02)	Large subunit ribosomal protein L29e	L29e
RP-L31e	Downregulated (-1.11)	Large subunit ribosomal protein L31e	L31e
RP-L35Ae	Downregulated (-1.12)	Large subunit ribosomal protein L35Ae	L35Ae
RP-L35e	Downregulated (-1.10)	Large subunit ribosomal protein L35e	L35e
RP-L37Ae	Downregulated (-1.92)	Large subunit ribosomal protein L37Ae	L37Ae
RP-L37e	Downregulated (-1.04)	Large subunit ribosomal protein L37e	L37e

RT-qPCR verification

We used RT-qPCR to verify four DEGs: two DEGs from osmoregulation-related pathways (*ATP1A* and *CLCN2*; Table 5) and two random DEGs in other pathways

(*HK* and *glyA*). Consistent with the RNA-seq results, RT-qPCR identified *ATP1A*, *CLCN2,* and *HK* (hexokinase) as significantly upregulated in the LS group as compared to the control (|log2FC| > 1 and FDR < 0.05; Fig 4). Although *glyA* (glycine hydroxymethyltransferase) was not significantly downregulated between the LS and control groups in the qRT-PCR analysis, this gene had similar patterns of expression in both the qRT-PCR and the RNA-Seq analyses (Fig 4).

Discussion

Assembly quality and GO classification

The *F. chinensis* transcriptome assembled in this study had an N50 of 1,004 bp, which was similar to, but slightly better than, those previously obtained for *P. vannamei* (448 bp; [23]) and *Oratosquilla oratoria* (798 bp; [45]). This indicated that our assembly was of acceptable quality. Consistent with previous studies of osmoregulation ([23-24]), the unigenes identified in this study were primarily associated with cation binding, macromolecule metabolic process, and organonitrogen compound metabolic process. This suggested that genes with functions in these categories are potentially important to adaptation to low-salinity environments. The result also partially supports the finding from Yuan (2017), who showed that 15.02 % and 16.24 % of positively selected genes in seawater and freshwater shrimps, respectively, enriched in the functions of cation binding; 22.71% and 18.80% positively selected genes in seawater and freshwater shrimps, respectively, enriched in the functions of cellular macromolecule metabolic process [46]. In their study, however, no specific and osmoregulation-related data for *F. chinensis* is available,

thus genes used in this study are not identical compared to that in their study. Whether unigens enriched in other GO terms mentioned by this study (Fig 1) have positive selection sites to adapt the low-salinity environments, which is another question to answer in future.

DEGs and pathways adapted to low salinity

Minerals not only serve as nutrients, but also are essential components of osmoregulation for crustaceans [3]. In the LS group, three genes in the mineral absorption pathway (ko04978) were differentially expressed as compared to the control: three were upregulated (*ATP1A*, *CLCN2*, and *HMOX2*), and one was downregulated (*SLC40A1/FPN1*; Table 5). Of these, *ATP1A*, *CLCN2,* and *SLC40A/FPN1* encode channel transporter proteins, while *HMOX2* encodes an intracellular protein. Our identification of these DEGs in this important pathway suggested that they may play a role in osmoregulation in response to low-salinity exposure.

ATP1A is involved in encoding a Na^+/K^+-ATPase that controls the movements of the Na^+ and K^+ ions between the hemolymph and the intracellular fluid [1]. The upregulation of Na^+/K^+-ATPase on the basolateral membrane causes more Na^+ ions to be transported out than K^+ ions taken in [47]. The upregulation of the chloride channel protein (encoded by *CLCN2*) has a similar effect on osmoregulation, increasing the amount of Cl^- leaving the cell and entering the hemolymph space. This process thus facilitates the rapid adaptation of *F. chinensis* to low-salinity environments by increasing salt concentration in hemolymph [1]. Indeed, previous studies have shown

301 that *F. chinensis* hemolymph is hyperosmotic to the external medium at low salinities
302 (e.g., 5 ppt) [10, 30]. On this point, the results support the opinion reviewed by
303 Péqueux (1995) and Henry (2012) that osmoregulators in low-salinity environment
304 (below 26 ppt) will turn on mechanisms of anisomotic extracelluar regulation to
305 stabilize hemolymph osmotic and ionic concentrations [1, 3]. Although the control
306 group (20 ppt) is already in low-salinity environment according to reference salinity
307 of 26 ppt, the result has implied that the salinity difference between 5 ppt and 20 ppt
308 is too huge enough to make their gene expression difference, as well as the
309 hemolymph osmolality [21].

310 We also observed that two genes associated with iron levels were differentially
311 expressed in the LS group as compared to the control: *HMOX2,* which encodes heme
312 oxygenase 2, was upregulated, and *SLC40A1/FPN1,* which encodes an iron-regulated
313 transporter, was downregulated. The differential expression of these genes may lead
314 to the increased production of ferrous irons and reduced iron outflow (ko04978) in the
315 LS group. A previous study had showed that the decreased iron concentration in blood
316 of *Cacinus maenas* was associated with their adaptation to osmotic stress [48]. The
317 downregulation of the iron-regulated transporter (DIRT) in this study has provided a
318 new interpretation that how the iron concentration in blood was decreased at the
319 molecular level. Besides the crustaceans, the DIRT even occurred in fish species like
320 steelhead trout (*Oncorhynchus mykiss*). However, fewer reports clearly showed the
321 function of the iron in osmoregulation [48-49]. Decreasing blood iron concentration in
322 crustaceans under salinity stress was interpreted by the sortation of iron from blood to

323 other tissues [48]. Moreover, extreme salinity stress will generates an increase in the
324 ROS (reactive oxygen species) which is harmful to crustaceans [3]. Iron in tissues
325 plays a role in oxidative metabolism by the form of a key competent in cytochromes
326 and enzymes [50]. Thus, taken together, it may be the way for *F. chinensis* in low
327 salinity in response to salinity stress that the iron in gill cells is prone to be used for
328 synthesis of bio-molecules (cytochromes and enzymes) involved in oxidative
329 metabolism.

330 In addition regulating salt and mineral levels, crustaceans maintain an
331 approximately constant osmotic concentration of extracellular fluid (hemolymph)
332 regardless of the salinity of the surrounding medium, by regulating water flow in and
333 out of the hemolymph [1]. Here, three unigenes in the vasopressin-regulated water
334 reabsorption pathway (ko04962; *AQP4*, *VAMP2*, and *RAB5*) were downregulated in
335 the LS group. We expect that this downregulation will reduce water inflow to the
336 hemolymph, helping to maintain a constant osmotic concentration. In particular,
337 because the primary function of AQP4 is to transport water across the plasma
338 membrane into hemolymph [19, 51], thus, the downregulation of the *AQP4* gene will
339 facilitate reduction of hemodilution. Similarly, the downregulation of *VAMP2* will
340 strongly inhibit AQP2 fusion at the apical membrane, which has been shown to
341 decrease water flow into the hemolymph in vertebrates [18, 52]. Finally, the
342 downregulation of *RAB5* may also inhibit the fusion of AQP2 at the endosomal apical
343 membrane; RAB5 is also one of the components implicated in early endosome fusion
344 [53], particularly, which is predicted to be involved in the regulation of AQP2

345 trafficking to and from the plasma membrane [54]. Thus, this study reports, for the
346 first time, that the genes (*AQP4*, *VAMP2*, and *RAB5*) are associated with the reduction
347 of water-permeability in *F. chinensis* in response to low-salinity environments.

348 In the study, we expected that the allostatic load on *F. chinensis* would increase
349 when salinity decreased from 20 ppt to 5 ppt. All forms of allostasis require energy, as
350 allostatic load increases, the amount of energy available for other biological functions
351 decreases [6, 21, 23, 25, 55]. We found that most of the DEGs in the ribosome
352 pathway (ko03010) were downregulated in the LS group as compared to the control
353 (Table 5). Ribosome is the location of polypeptide synthesis. Downregulation of the
354 structural macromolecular components in ribosome could decrease polypeptide
355 synthesis. The previous study showed proteins L4, L22, L39e, L19, L23, L24, L29
356 and L31e are important to polypeptide synthesis [56]. Downregulation of these genes
357 in this study implies the synthesis of proteins will be affected in *F. chinensis* exposed
358 to low salinities. Notably, it seems that proteins not involved in low-salinity resistance
359 more likely decrease, concomitant with the diversion of energy resources to
360 osmoregulation. Similarly, *P. vannamei* subjected to chronic low-salinity stress
361 upregulated the expression of AMP-activated protein kinase (AMPK) to maintain
362 energy balance by increasing catabolism to generate ATP and decreasing anabolism to
363 conserve ATP [57]. However, *AMPK* was not significantly differentially expressed in
364 *F. chinensis*. This suggested that, unlike *P. vannamei* (another common shrimp
365 species cultured in China), *F. chinensis* may not have a strong ability to adapt to
366 low-salinity conditions in maintaining energy balance. Otherwise, another evidence

367 implying the weaker adaption of *F. chinensis* to low salinity compared to *P. vannamei*
368 can be found in studies from Tang (2016) and Li (2019b) [21, 26]. Hemolymph
369 osmolality of *F. chinensis* was significantly reduced when salinity decreased from 15
370 ppt to 10 ppt [21], while that of *P. vannamei* did not significantly reduced even when
371 environmental salinity decreased from 12 ppt to 0 ppt [26]. Thus, successfully
372 low-salinity aquaculture of *F. chinensis* deserves more attention.

373 In this study, we used two different salinities to identify DEGs potentially
374 associated with the response of *F. chinensis* to low salinity. Because we only
375 compared two salinities, our results do not reflect the adaptation process. To better
376 understand the mechanisms associated with gradual or continuous changes in salinity,
377 we aim to investigate the responses of this species to additional salinities in future
378 studies, using both RNA-Seq and RT-qPCR.

379 In summary, our results indicated that four unigenes in the mineral absorption
380 pathway (*ATP1A*, *CLCN2*, *HMOX2,* and *SLC40A1/FPN1*), as well as three unigenes
381 in the vasopressin-regulated water reabsorption pathway (*AQP4*, *VAMP2*, and *RAB5*),
382 were differentially expressed in *F. chinensis* in response to low-salinity exposure.
383 These pathways, in conjunction with the ribosome pathway, may be important for
384 osmoregulation in *F. chinensis* under low-salinity conditions. Although the associated
385 mechanisms require further investigation, our results help to clarify the molecular
386 responses of *F. chinensis* to low-salinity environments. This study suggests that *F.*
387 *chinensis* could be an evolutionary model of weake osmoregulator, combining with
388 patterns of hemolymph osmoregulation (include the strong osmoregulator, weak

389 osmoregulator and osmoconformer, etc.) in aquatic crustaceans viewed by Péqueux
390 (1995) [1].

391 Data Availability Statement

392 The raw data have been uploaded to SRA database (PRJNA669213).

393 Funding

394 The work was funded by Natural Science Foundation of the Jiangsu Higher
395 Education Institutions of China (19KJD180001); and sponsored by "Qing Lan Project
396 of Jiangsu Province of China"; Young Talents Support Program in Lianyungang
397 Normal College (LSZQNXM201702); Open Foundation of Jiangsu Key Laboratory
398 for Bioresources of Saline Soils (JKLBS2016008).

399 Acknowledgements

400 We thank LetPub (www.letpub.com) for its linguistic assistance and scientific
401 consultation during the preparation of this manuscript.

402 Author Contributions

403 **Data curation**: Lei Zhang, Zhengfei Wang.

404 **Funding acquisition**: Jun Liu.

405 **Resources**: Shiguang Shao, Lei Zhang.

406 **Writing – original draft**: Jun Liu, Jie Shen.

407 **Writing – review & editing**: Jun Liu, Jie Shen, Daizhen Zhang.

408 Competing Interests

409 The authors have declared that no competing interests exist.

410

411

412 # References

413 **1**. Péqueux A. Osmotic regulation in crustaceans. Journal of Crustacean Biology.
414 1995; 15(1): 1-60. https://doi.org/10.2307/1549010

415 **2**. Foster C, Amado EM, Souza MM, Freire CA. Do osmoregulators have lower
416 capacity of muscle water regulation than osmoconformers? A study on decapod
417 crustaceans. Journal of Experimental Zoology Part A: Ecological Genetics and
418 Physiology. 2010; 313A(2): 80-94. https://doi.org/10.1002/jez.575

419 **3**. Henry RP, Lucu C, Onken H, Weihrauch D. Multiple functions of the crustacean
420 gill: osmotic/ionic regulation, acid-base balance, ammonia excretion, and
421 bioaccumulation of toxic metals. Frontiers in physiology. 2012; 3: 1-33.
422 https://doi.org/10.3389/fphys.2012.00431

423 **4**. McNamara JC, Faria SC. Evolution of osmoregulatory patterns and gill ion
424 transport mechanisms in the decapod Crustacea: a review. Journal of
425 Comparative Physiology B: Biochemical, Systemic & Environmental Physiology.
426 2012; 182(8): 997-1014. https://doi.org/10.1007/s00360-012-0665-8

427 **5**. Henry RP. Environmentally mediated carbonic anhydrase induction in the gills of
428 euryhaline crustaceans. The Journal of Experimental Biology. 2001; 204(5):
429 991-1002.

430 **6**. Sundell K, Wrange AL, Jonsson PR, Blomberg A. Osmoregulation in barnacles:
431 An evolutionary perspective of potential mechanisms and future research
432 directions. Frontiers in Physiology. 2019; 10: 877.
433 https://doi.org/10.3389/fphys.2019.00877

434 **7**. Li E, Chen L, Zeng C, Yu N, Xiong Z, Chen X, et al. Comparison of digestive and
435 antioxidant enzymes activities, haemolymph oxyhemocyanin contents and

436 hepatopancreas histology of white shrimp, *Litopenaeus vannamei*, at various
437 salinities. Aquaculture, 2008; 274(1): 80-86.
438 https://doi.org/10.1016/j.aquaculture.2007.11.001

439 **8**. Bonilla-Gómez JL, Chiappa-Carrara X, Galindo C, Jeronimo G, Cuzon G, Gaxiola
440 G. Physiological and biochemical changes of wild and cultivated juvenile pink
441 shrimp *Farfantepenaeus duorarum* (Crustacea: Penaeidae) during molt cycle.
442 Journal of Crustacean Biology. 2012; 32(4): 597-606. https://doi.org/
443 10.1163/193724012X630679

444 **9**. Havird JC, Mitchell RT, Henry RP, Santos SR. Salinity-induced changes in gene
445 expression from anterior and posterior gills of *Callinectes sapidus* (Crustacea:
446 Portunidae) with implications for crustacean ecological genomics. Comparative
447 Biochemistry and Physiology Part D: Genomics and Proteomics. 2016; 19(C),
448 34-44. https://doi.org/10.1016/j.cbd.2016.06.002

449 **10**. Li J, Li W, Zhang X. Effects of dissolved oxygen, starvation, temperature, and
450 salinity on the locomotive ability of juvenile Chinese shrimp *Fenneropenaeus*
451 *chinensis*. Ethology Ecology & Evolution. 2019a; 31(2): 155-172.
452 https://doi.org/10.1080/03949370.2018.1526215

453 **11**. Cameron JN, Batterton CV. Antennal gland functionin the freshwater bluecrab,
454 *Callinectes sapidus*: water, electrolyte, acid-base and ammonia excretion. Journal
455 of Comparative Physiology. 1978a; 123: 143-148.
456 https://doi.org/10.1007/BF00687842

457 **12**. Cameron JN, Batterton CV. Temperature and blood acid-basse status in the blue
458 crab, *Callinectes sapidus*. Respiration physiology. 1978b; 35(2): 101-110.
459 https://doi.org/10.1016/0034-5687(78)90015-4 PMID: 33428

460 **13**. Neufeld GJ, Pritchard JB. Osmoregulation and gill Na, K-ATPase in the rock crab,

Cancer irroratus: response to DDT. Comparative biochemistry and physiology. C: Comparative pharmacology. 1979; 62c(2): 165-172. https://doi.org/10.1016/0306-4492(79)90005-4

14. Henry RP, Cameron JN. The distribution and partial characterization of carbonic anhydrase in selected aquatic and terrestrial decapod crustaceans. Journal of Experimental Zoology. 1982; 221: 309-321. https://doi.org/10.1002/jez.1402210306

15. Varley DG, Greenaway P. Nitrogenous excretion in the terrestrial carnivorous crab *geograpsus grayi*: site and mechanism of excretion. The Journal of Experimental Biology. 1994; 190(1): 179-193.

16. Chung JS, Maurer L, Bratcher M, Pitula JS, Ogburn MB. Cloning of aquaporin-1 of the blue crab, *Callinectes sapidus*: its expression during the larval development in hyposalinity. Aquatic Biosystems. 2012; 8(1), 21. https://doi.org/10.1186/2046-9063-8-21

17. Nejsum LN, Zelenina M, Aperia A, Frokiaer J, Nielsen S. Bidirectional regulation of AQP2 traffcking and recycling: involvement of AQP2-S256 phosphorylation. American Journal of Physiology: Renal Physiology. 2005; 288: F930-F938. https://doi.org/10.1152/ajprenal.00291.2004

18. Campbell EM, Ball A, Hoppler S, Bowman AS. Invertebrate aquaporins: a review. Journal of Comparative Physiology B: Biochemical, Systemic, and Environmental Physiology. 2008; 178(8): 935-955. https://doi.org/10.1007/s00360-008-0288-2

19. Ishibashi K, Sasaki S. Aquaporin water channels in mammals. Clinical and Experimental Nephrology. 1997; 1(4): 247-253. https://doi.org/10.1007/BF02480636

20. Chen JC, Lin JN. Osmolality and chloride concentration in the hemolymph of subadult *Penaeus chinensis* subjected to different salinity levels. Aquaculture. 1994; 125(1-2): 167-174. https://doi.org/10.1016/0044-8486(94)90293-3

21. Li J, Xu X, Li W, Zhang X. Linking energy metabolism and locomotor variation to osmoregulation in Chinese shrimp *Fenneropenaeus chinensis*. Comparative Biochemistry and Physiology Part - B: Biochemistry and Molecular Biology. 2019b; 234: 58-67. https://doi.org/10.1016/j.cbpb.2019.05.006

22. Péqueux A, Gilles R. NaCl transport in gills and related structures. Part I: Invertebrates. In: Advances in Comparative and Environmental Physiology (Gerger R, ed.), 1988; pp 2-47. Springer-Verlag, Berlin, Germany.

23. Zhang D, Wang F, Dong S, Lu Y. De novo assembly and transcriptome analysis of osmoregulation in *Litopenaeus vannamei* under three cultivated conditions with different salinities. Gene. 2016; 578(2): 185-193. https://doi.org/10.1016/j.gene.2015.12.026

24. Zhang D, Liu J, Qi T, Ge B, Liu Q, Jiang S, et al. Comparative transcriptome analysis of *Eriocheir japonica sinensis* response to environmental salinity. PLoS ONE, 2018a; 13(9): e0203280. https://doi.org/10.1371/journal.pone.0203280 PMID: 30192896

25. Gao B, Sun D, Lv J, Ren X, Liu P. Li J. Transcriptomic analysis provides insight into the mechanism of salinity adjustment in swimming crab *Portumus trituberculatus*. Genes and Genomics. 2019; 41(8): 961-971. https://doi.org/10.1007/s13258-019-00828-4

26. Tang JZ, Liu Z, Wang XL, Qi SW, Bai LY, Zhang JC, et al. Effects of desalination on survival rate, osmolality and Na+ / K+-ATPase activity of *Penaeus vannamei*. Freshwater Fisheries. 2016; 46(3): 82-86.

511 **27**. Liu B, Yu Z, Song X, Guan Y, Jian X, He J. The effect of acute salinity change on
512 white spot syndrome (WSS) outbreaks in *Fenneropenaeus chinensis*.
513 Aquaculture. 2006; 253(1-4): 163-170.
514 https://doi.org/10.1016/j.aquaculture.2005.08.022
515 **28**. Sen D, Fang W, Hao S, Biao G, Shuanglin D. Effects of salinity fluctuation
516 frequency on the osmolarity, Na^+-K^+-ATPase activity and hsp70 expression in
517 juvenile chinese shrimp, *Fenneropenaeus chinensis*. Journal of Ocean University
518 of China. 2009; 8(1): 71-76. 10.1007/s11802-009-0071-3
519 **29**. Pan L, Li L, Zhang L. Variations of ion-transport enzyme activities during early
520 development of the shrimps *Fenneropenaeus chinensis* and *Marsupenaeus*
521 *japonicus*. Journal of Ocean University of China, 2010; 9(1): 76-80.
522 https://doi.org/10.1007/s11802-010-0076-y
523 **30**. Chen JC, Lin MN, Ting YY, Lin JN. Survival, haemolymph osmolality and tissue
524 water *Penaeus chinensis* juveniles acclimated to different salinity and
525 temperature levels. Comparative Biochemistry and Physiology - A Physiology.
526 1995; 110(3): 253-258. https://doi.org/10.1016/0300-9629(94)00164-O
527 **31**. Cock PJA, Fields CJ, Goto N, Heuer ML, Rice PM. The Sanger FASTQ file
528 format for sequences with quality scores, and the Solexa/Illumina FASTQ
529 variants. Nucleic Acids Research. 2010; 38(6): 1767-1771.
530 https://doi.org/10.1093/nar/gkp1137 PMID: 20015970
531 **32**. Martin M. Cutadapt removes adapter sequences from high-throughput sequencing
532 reads. *Embnet Journal*, 2011; 17: 10-12. https://doi.org/10.14806/ej.17.1.200
533 **33**. Haas BJ, Papanicolaou A, Yassour M, Grabherr M, Blood PD, Bowden J, et al.
534 De novo transcript sequence reconstruction from RNA-seq using the Trinity
535 platform for reference generation and analysis. Nature Protocols. 2013; 8(8):

536 1494-512. https://doi.org/10.1038/nprot.2013.084

537 **34**. Nadia M, Davidson AO. Corset: enabling differential gene expression analysis for
538 de novo assembled transcriptomes. Genome Biology. 2014; 15(7): 410.
539 https://doi.org/10.1186/s13059-014-0410-6

540 **35**. Altschul SF, Gish W, Miller W, Myers EW, Lipmanl DJ. Basic local alignment
541 search tool. Journal of Molecular Biology. 1990; 215(3): 403-410.
542 https://doi.org/10.1016/S0022-2836(05)80360-2

543 **36**. Conesa A, Gotz S, Garcia-Gomez JM, Terol J, Talon M, Rob-les M. Blast2GO: a
544 universal tool for annotation, visualization and analysis in functional genomics
545 research. Bioinformatics. 2005; 21(18): 3674-3676.
546 https://doi.org/10.1093/bioinformatics/bti610

547 **37**. Li B, Dewey CN. RSEM: accurate transcript quantification from RNA-seq data
548 with or without a reference genome. BMC Bioinformatics. 2011; 12(1): 323.
549 https://doi.org/10.1186/1471-2105-12-323

550 **38**. Reiner A, Yekutieli D, Benjamini Y. Identifying differentially expressed genes
551 using false discovery rate controlling procedures. Bioinformatics. 2003; 19(3):
552 368-375. https://doi.org/10.1093/bioinformatics/btf877

553 **39**. Trapnell C, Hendrickson DG, Sauvageau M, Goff L, Rinn JL, Pachter L.
554 Differential analysis of gene regulation at transcript resolution with RNA-seq.
555 Nature Biotechnology. 2013; 31(1): 46-53. https://doi.org/10.1038/nbt.2450
556 PMID: 23222703

557 **40**. Li Y, Wang X, Li C, Hu S, Yu J, Song S. Transcriptome-wide
558 n6-methyladenosine profiling of rice callus and leaf reveals the presence of
559 tissue-specific competitors involved in selective mRNA modification. RNA
560 Biology. 2014; 11(9): 1180-1188. https://doi.org/10.4161/rna.36281

561 **41**. Lalitha S. Primer premier 5. Biotech Software & Internet Report. 2000; 1:
562 270-272. https://doi.org/10.1089/152791600459894
563 **42**. Wang S, Wang Y, Wu H, Hu L. Rbp2 induces epithelial-mesenchymal transition
564 in non-small cell lung cancer. Plos One. 2013; 8(12): e84735.
565 https://doi.org/10.1371/journal.pone.0084735
566 **43**. Liao P, Satten GA, Hu YJ. PhredEM: a phred-score-informed genotype-calling
567 approach for next-generation sequencing studies. Genetic Epidemiology. 2017;
568 7(5): 1393-1404. https://doi.org/10.1002/gepi.22048
569 **44**. Miller JR, Koren S, Sutton G. Assembly algorithms for next-generation
570 sequencing data. Genomics. 2010; 95(6): 315-327.
571 https://doi.org/10.1016/j.ygeno.2010.03.001
572 **45**. Zhang D, Liu J, Qi T, Ge B, Wang Z, Jiang S, et al. Transcriptome analysis of
573 hepatopancreas from the Cr (VI)-stimulated mantis shrimp (*Oratosquilla*
574 *oratoria*) by illumina paired-end sequencing: Assembly, annotation, and
575 expression analysis. Journal of Agricultural and Food Chemistry. 2018b; 66(11):
576 2598-2606. https://doi.org/10.1021/acs.jafc.7b05074
577 **46**. Yuan J, Zhang X, Liu C, Duan H, Li F, Xiang J. Convergent evolution of the
578 osmoregulation system in decapod shrimps. Marine Biotechnology. 2017; 19(1):
579 76-88. https://doi.org/10.1007/s10126-017-9729-9
580 **47**. Lingrel JB. Na, K-ATPase: isoform structure, function, and expression. Journal of
581 Bioenergetics & Biomembranes. 1992; 24(3): 263-270.
582 https://doi.org/10.1007/BF00768847
583 **48**. Spaargaren DH. Osmotically induced changes in copper and iron concentrations in
584 three euryhaline crustacean species. Netherlands Journal of Sea Research. 1983;
585 17: 96-105.

586 **49**. Xiong Y, Dong S, Huang M, Li Y, Zhou Y. Growth, osmoregulatory response,
587 adenine nucleotide contents, and liver transcriptome analysis of steelhead trout
588 (*Oncorhynchus mykiss*) under different salinity acclimation methods.
589 Aquaculture. 2020; 520: 734937.
590 https://doi.org/10.1016/j.aquaculture.2020.734937
591 **50**. King EN. Oxidative activity of crab gill mitochondria as a function of osmotic
592 concentration. Comparative Biochemistry and Physiology. 1966; 17(1): 245-258.
593 https://doi.org/10.1016/0010-406X(66)90024-7
594 **51**. Ishibashi K, Hara S, Kondo S. Aquaporin water channels in mammals. Clinical
595 and Experimental Nephrology. 2009; 13(4): 107-117.
596 https://doi.org/10.1007/BF02480636
597 **52**. Procino G, Barbieri C, Tamma G, De Benedictis L, Pessin JE, Svelto M. et al.
598 AQP2 exocytosis in the renal collecting duct - involvement of SNARE isoforms
599 and the regulatory role of Munc18b. Journal of Cell Science. 2008; 121(12):
600 2097-2106. https://doi.org/10.1242/jcs.022210
601 **53**. Navaroli DM, Bellvé KD, Standley C, Lifshitz LM, Cardia J, Lambright D, et al.
602 Rabenosyn-5 defines the fate of the transferrin receptor following
603 clathrin-mediated endocytosis. Proceedings of the National Academy of Sciences
604 of the United States of America. 2012; 109(8): E471–E480.
605 https://doi.org/10.1073/pnas.1115495109
606 **54**. Procino G, Barbieri C, Carmosino M, Tamma G, Milano S, De Benedictis L, et al.
607 Fluvastatin modulates renal water reabsorption in vivo through increased AQP2
608 availability at the apical plasma membrane of collecting duct cells. *Pflügers*
609 *Archiv - European Journal of Physiology*, 2011; 462(5): 753-766.
610 https://doi.org/10.1007/s00424-011-1007-5

611 **55**. Bett C, Vinatea L. Combined effect of body weight, temperature and salinity on
612 shrimp *Litopenaeus vannamei* oxygen consumption rate. Brazilian Journal of
613 Oceanography. 2009; 57(4): 305-314.
614 https://doi.org/10.1590/S1679-87592009000400005
615 **56**. Nissen P, Hansen J, Ban N, Moore PB, Steitz TA. The structural basis of
616 ribosome activity in peptide bond synthesis. Science, 2000; 289(5481): 920-930.
617 https://doi.org/10.1126/science.289.5481.920
618 **57**. Xu C, Li E, Xu Z, Wang S, Chen K, Wang X, et al. Molecular characterization
619 and expression of AMP-activated protein kinase in response to low-salinity stress
620 in the Pacific white shrimp *Litopenaeus vannamei*. Comparative Biochemistry
621 and Physiology Part - B: Biochemistry and Molecular Biology. 2016; 198:
622 79-90.
623

624 **Fig 1.** Gene Ontology (GO) analysis of the unigenes in the *Fenneropenaeus chinensis*
625 genome, showing the GO terms most overrepresented in the GO categories (**A)**
626 biological processes, (**B**) cellular components, and (**C**) molecular function. The colors
627 in each pie chart correspond to GO terms, and the size of each slice represents the
628 proportion of unigenes associated with each GO term.

629

630 **Fig 2.** Unigene expression patterns. The horizontal and vertical axes present the
631 expression levels of unigenes in the two groups (TPM, transcripts per kilobase
632 million, values); each value was logarithmically transformed. DEGs, i.e., unigenes
633 with expression fold changes | log2FC| > 1 and FDR < 0.05, are marked with red and
634 blue. Red dots represent unigenes that were significantly upregulated under low
635 salinity, blue dots represent those that were significantly downregulated under low
636 salinity, and black dots represent genes that are not DEGs. The greater the deviation
637 of a dot from the diagonal, the greater the difference in the unigene expression
638 between the two groups. Dots near 0 represent unigenes with low expression.

639

640 **Fig 3.** KEGG (Kyoto Encyclopedia of Genes and Genomes) pathways significantly
641 enriched in the DEGs. Each bar represents a pathway, and the height of bar reflects
642 the enrichment ratio (equal to Sample Number / Background Number). *: FDR <
643 0.05, **: FDR < 0.01.

644

645 **Fig 4.** RT-qPCR verification of four representative genes (*ATP1A, CLCN2*, *HK,* and
646 *glyA*) identified as differentially expressed between low-salinity and control groups of
647 *Fenneropenaeus chinensis.* *: FDR < 0.05. Each bar with standard error represents
648 three replicates.

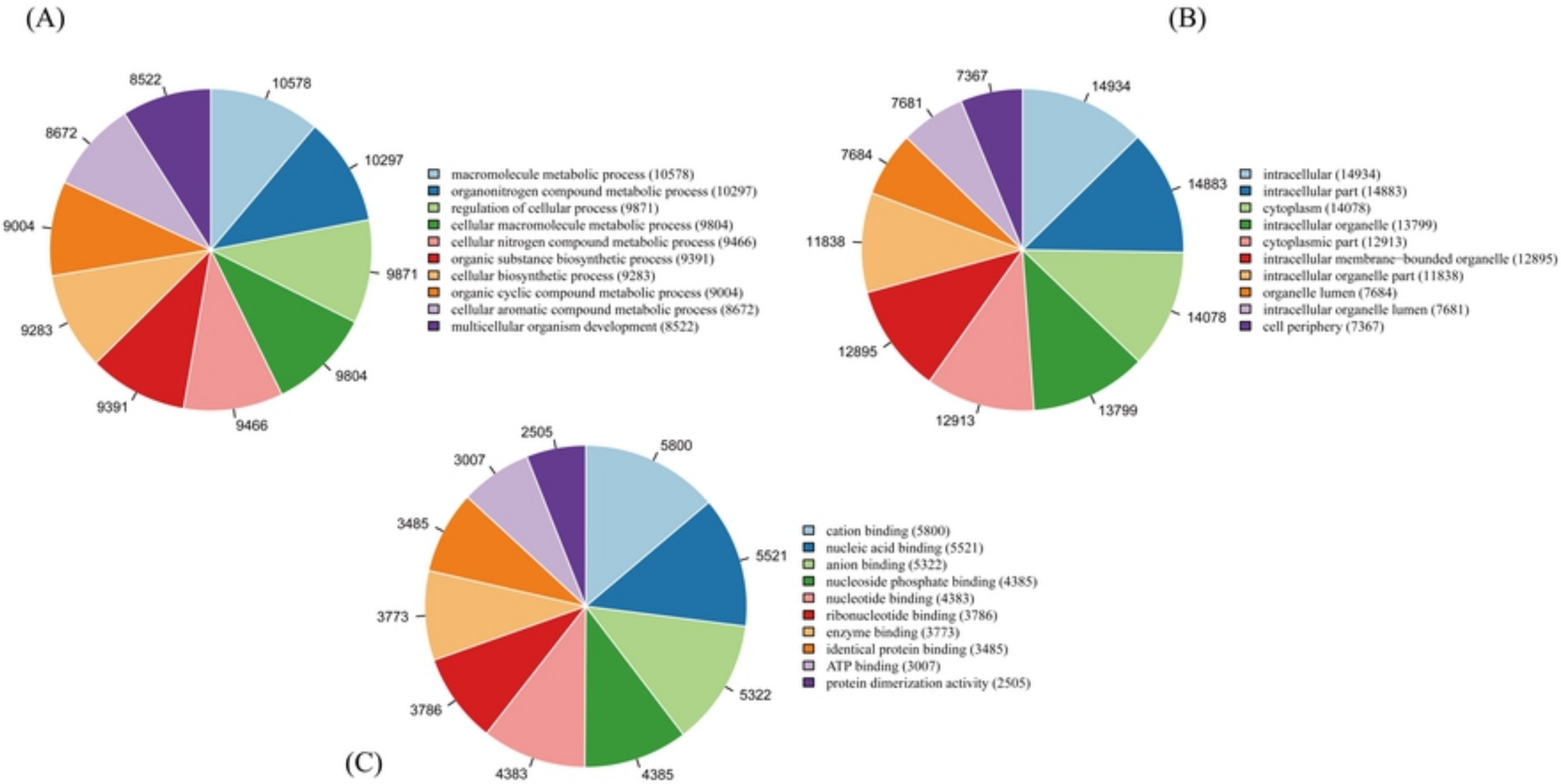
(A)
10578
10297
9871
9804
9466
9391
9283
9004
8672
8522
macromolecule metabolic process (10578)
organonitrogen compound metabolic process (10297)
regulation of cellular process (9871)
cellular macromolecule metabolic process (9804)
cellular nitrogen compound metabolic process (9466)
organic substance biosynthetic process (9391)
cellular biosynthetic process (9283)
organic cyclic compound metabolic process (9004)
cellular aromatic compound metabolic process (8672)
multicellular organism development (8522)
(B)
14934
14883
14078
13799
12913
12895
11838
7684
7681
7367
intracellular (14934)
intracellular part (14883)
cytoplasm (14078)
intracellular organelle (13799)
cytoplasmic part (12913)
intracellular membrane−bounded organelle (12895)
intracellular organelle part (11838)
organelle lumen (7684)
intracellular organelle lumen (7681)
cell periphery (7367)
(C)
5800
5521
5322
4385
4383
3786
3773
3485
3007
2505
cation binding (5800)
nucleic acid binding (5521)
anion binding (5322)
nucleoside phosphate binding (4385)
nucleotide binding (4383)
ribonucleotide binding (3786)
enzyme binding (3773)
identical protein binding (3485)
ATP binding (3007)
protein dimerization activity (2505)

Figure 1

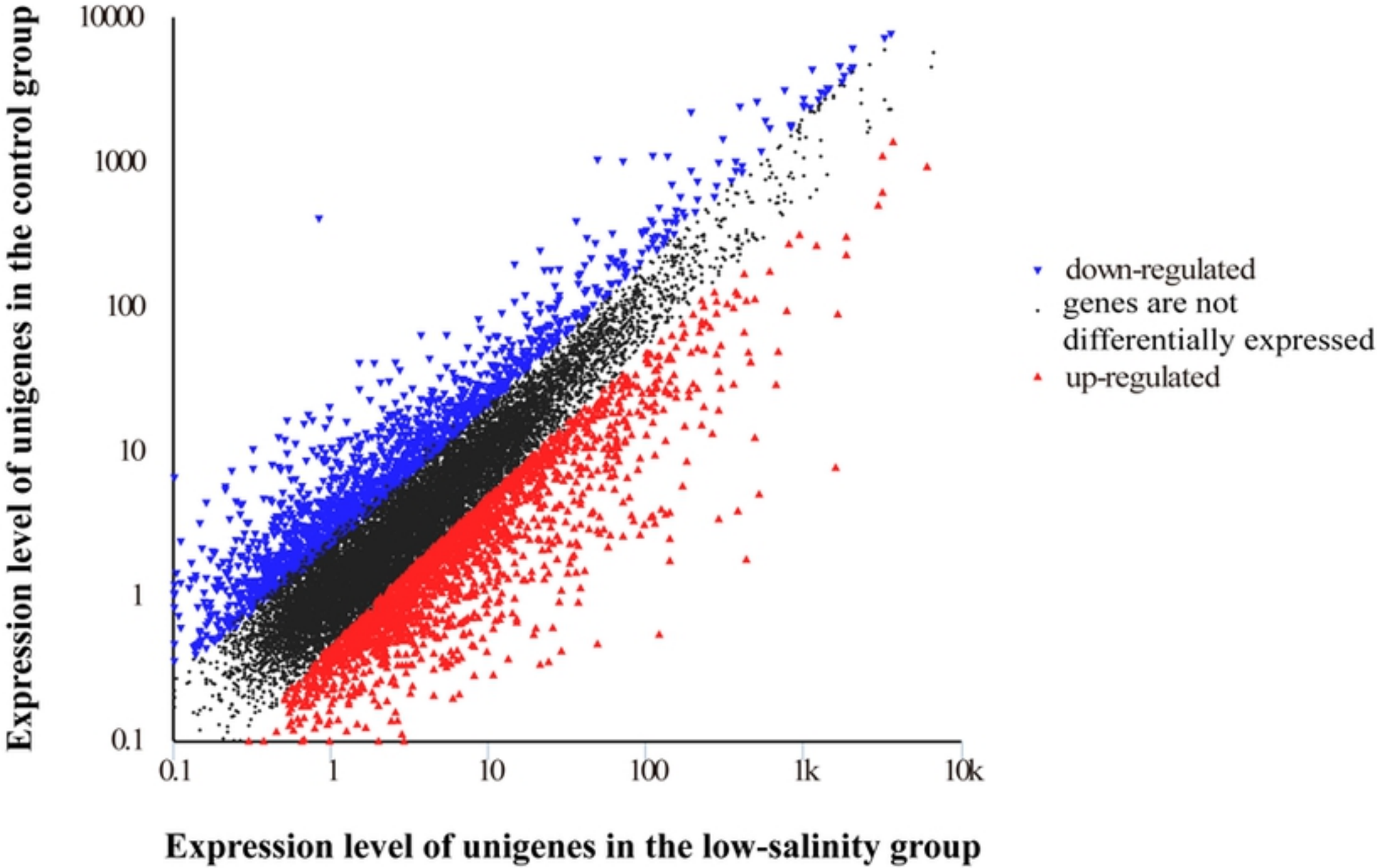
Expression level of unigenes in the control group
10000
1000
100
10
1
0.1
0.1
1
10
100
1k
10k
Expression level of unigenes in the low-salinity group
down-regulated
genes are not differentially expressed
up-regulated

Figure 2

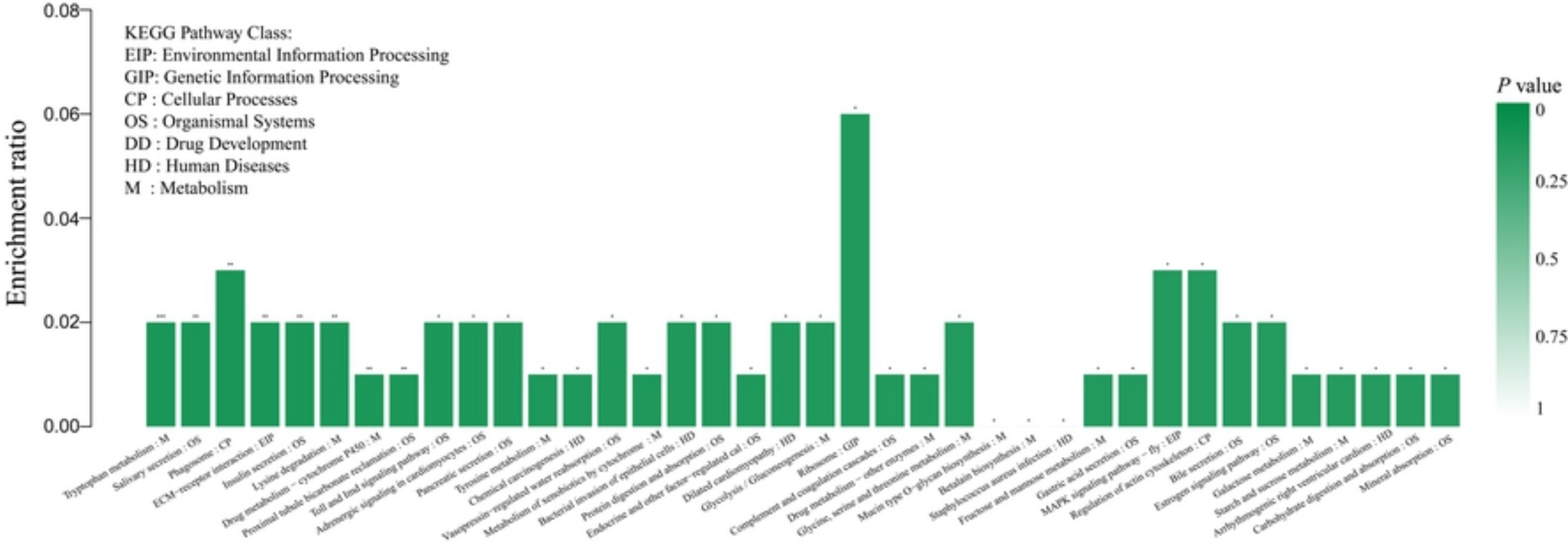
KEGG Pathway Class:
EIP: Environmental Information Processing
GIP: Genetic Information Processing
CP : Cellular Processes
OS : Organismal Systems
DD : Drug Development
HD : Human Diseases
M : Metabolism
Enrichment ratio
0.08
0.06
0.04
0.02
0.00
P value
0
0.25
0.5
0.75
1
Tryptophan metabolism : M
Salivary secretion : OS
Phagosome : CP
ECM−receptor interaction : EIP
Insulin secretion : OS
Lysine degradation : M
Drug metabolism − cytochrome P450 : M
Proximal tubule bicarbonate reclamation : OS
Toll and Imd signaling pathway : OS
Adrenergic signaling in cardiomyocytes : OS
Pancreatic secretion : OS
Tyrosine metabolism : M
Chemical carcinogenesis : HD
Vasopressin−regulated water reabsorption : OS
Metabolism of xenobiotics by cytochrome : M
Bacterial invasion of epithelial cells : HD
Protein digestion and absorption : OS
Endocrine and other factor−regulated cal : OS
Dilated cardiomyopathy : HD
Glycolysis / Gluconeogenesis : M
Ribosome : GIP
Complement and coagulation cascades : OS
Drug metabolism − other enzymes : M
Glycine, serine and threonine metabolism : M
Mucin type O−glycan biosynthesis : M
Betalain biosynthesis : M
Staphylococcus aureus infection : HD
Fructose and mannose metabolism : M
Gastric acid secretion : OS
MAPK signaling pathway − fly : EIP
Regulation of actin cytoskeleton : CP
Bile secretion : OS
Estrogen signaling pathway : OS
Galactose metabolism : M
Starch and sucrose metabolism : M
Arrhythmogenic right ventricular cardiom : HD
Carbohydrate digestion and absorption : OS
Mineral absorption : OS

Figure 3

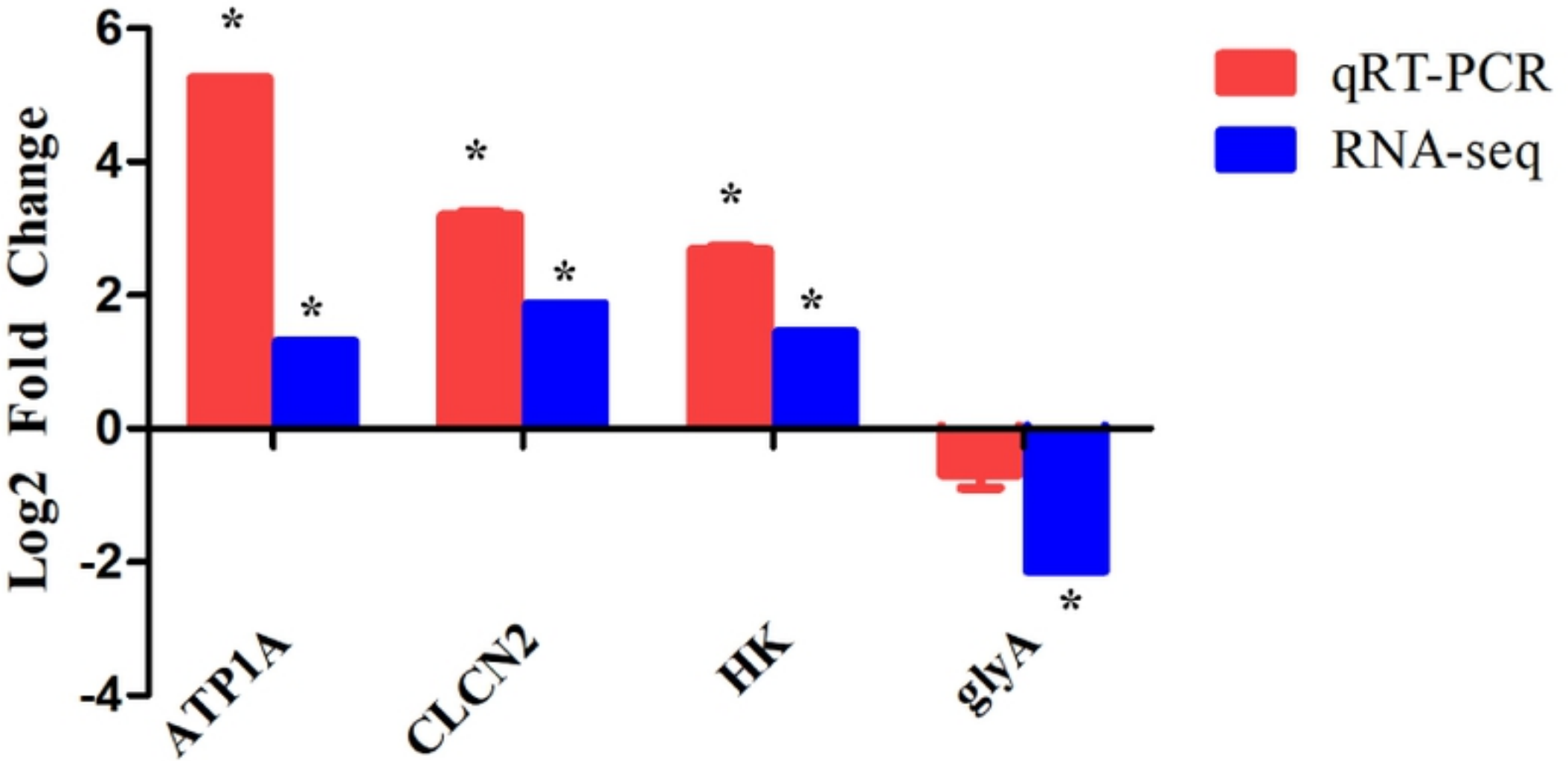

Figure 4